Time–Temperature–Transformation Diagram for Reactive Processing of Polyamide 12

A. LUISIER, P.-E. BOURBAN, J.-A. E. MÅNSON

Laboratoire de Technologie des Composites et Polymères (LTC), École Polytechnique Fédérale de Lausanne (EPFL), CH-1015 Lausanne, Switzerland

Received 13 March 2000; accepted 2 October 2000

ABSTRACT: In order to describe the different events occurring during the anionic polymerization of polyamide 12 (PA12), a general concept of a time, temperature, and transformation (TTT) diagram was established and related to reactive processing conditions. Polymerization kinetics were established, and it was found that the reaction was best described by an autocatalytic expression. Polymerization temperatures above and below the final polymer melting temperature were considered. Furthermore, the variation of the melting temperature and viscosity were followed as a function of the polymerization time and degree of conversion. It was shown that monomer–polymer phase separation and crystallization may occur during PA12 polymerization. The results could be adapted for use during liquid molding of PA12 polymers and their composites. © 2001 John Wiley & Sons, Inc. J Appl Polym Sci 81: 963–972, 2001

Key words: polyamide 12; thermoplastic composites; polymerization; crystallization; time–temperature–transformation diagram

INTRODUCTION

A major difficulty in processing thermoplastic composites is to achieve cost-effective high-quality impregnation of the fiber reinforcement by the matrix resin.[1] Unlike thermoset resins impregnation with thermoplastic resins is usually performed in their polymerized form, and difficulties with the impregnation arise from their high melt viscosity. A promising processing route for thermoplastic composites is to exploit very low monomer viscosity to achieve good fiber impregnation prior to *in situ* polymerization.

Different types of *in situ* polymerization have been studied. Up to now, polymerization of poly(methyl methacrylate),[2] linear polyurethane,[3] polystyrene,[4] and polyamide 6 (PA6)[5–8] have been investigated. The process requirements for these reactions are the following:

1. the initial viscosity of the reactants should be low to facilitate impregnation,
2. the reactants should be stable during storage,
3. the reaction should proceed at a cost-effective rate and without by-products, and
4. the final material should have a modulus and strength high enough to obtain good mechanical properties.

The first anionic polymerization of lactam (the monomer of PA) was reported by Joyce and Ritter in 1941.[9] Although the reaction feasibility was known for a long time, there is still only limited

Correspondence to: J.-A. E. Månson.

Contract grant sponsor: EMS CHEMIE AG and EBO; contract grant number: EUREKA project EU 1458-POLITE.

Contract grant sponsor: Commission for Technology and Innovation.

Journal of Applied Polymer Science, Vol. 81, 963–972 (2001)

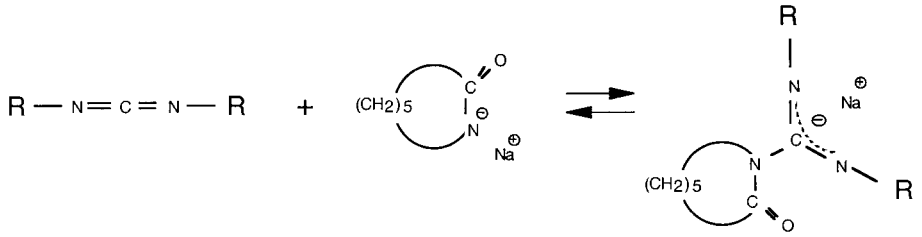

Figure 1 Guanidine anion formation from the activator and catalyst reaction. The three chemical species in the solvent will be referred to as the liquid system.

industrial exploitation. This article presents a new reactive system that allows infinite storage of the reactant and describes the different material transformations that appear during polymerization at different temperatures. Time–temperature–transformation (TTT) diagrams similar to that of thermosets[10] are developed here for thermoplastics. The TTT diagrams for thermosets provide an intellectual framework for understanding the curing process and are used to optimize the cure path and final material properties.[11] The goal of this study is to offer a map of the events that appear during polymerization of thermoplastics and to study their influence on the polymerization kinetics and the final degree of conversion achieved. Time–temperature routes could thus be provided to exploit *in situ* polymerization with various processing techniques such as reaction injection molding (RIM), rotomolding, resin transfer molding,[12] and pultrusion.

EXPERIMENTAL

Chemistry

In all previous studies, the anionic polymerization of PAs was initiated by mixing together a monomer batch containing an activator and a monomer batch containing a catalyst. These batches had a limited shelf life. In this work a patented liquid system[13] containing both the activator and the catalyst in a solvent was used. Because neither the activator nor the catalyst was in contact with the monomer, they could be stored indefinitely.

The anionic PA12 polymerization mechanisms involved the initial formation of a guanidine anion in the liquid system and during polymerization (Fig. 1). This anion was the product of a reaction between the activator (a carbodiimide) and the catalyst (the sodium-caprolactam). The fast initiation step of the polymerization corresponded to the reaction of the guanidine with the first monomer. The initiation was fast because the product (the new anion) was stabilized by resonance. Once formed, the new anion underwent rapid proton transfer and propagation (Fig. 2) by successive formation of resonance stabilized anions. The lactam anion is a catalyst because it was successively reformed. The carbodiimide is designated an activator because it significantly enhanced the effect of the catalyst during the initiation step by resonance stabilization.

Polymerization Kinetics

The polymerization was exothermic and a differential scanning calorimeter (Perkin–Elmer DSC7) was used to measure the reaction heat flow versus time at different constant temperatures. We calculated the reaction rate ($d\beta/dt$) by assuming a direct proportionality between the heat flow rate (dH/dt) and the $d\beta/dt$:

$$\frac{d\beta}{dt} = \frac{dH/dt}{\Delta H_o} \tag{1}$$

where ΔH_o is the overall heat of the reaction.

The activator and catalyst were added to the molten monomer just above its melting point and then cooled to room temperature to stop the reaction. The cold (crystallized) mixture was then sealed in DSC caps under a dry and oxygen-free atmosphere. These measurements were performed at several temperatures.

Chemorheology

The polymerization in this work had to be protected against oxygen and hydrous traces that react with the anions. The viscosity measurements were thus performed with a setup protecting the polymerization from the surrounding

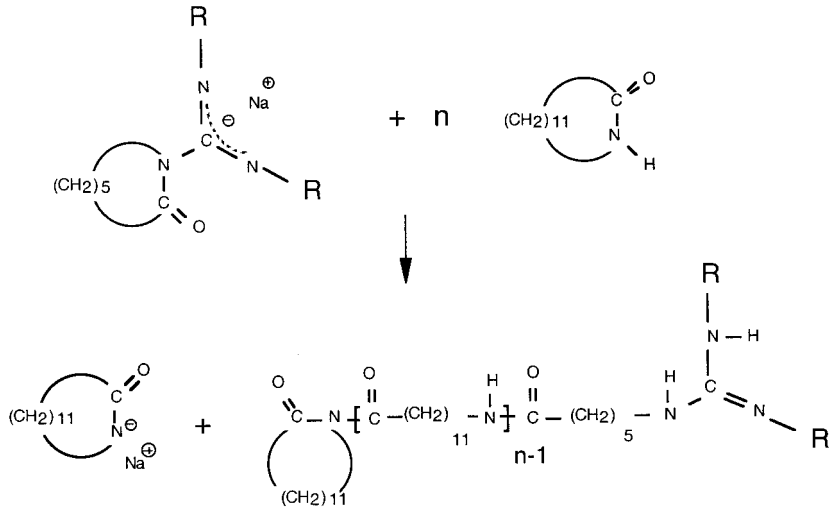

Figure 2 Polymerization mechanisms from the guanidine anion of the liquid system to the polymer end product. The monomer involved was laurillactam.

air.[14] The setup was a couette geometry with a friction free sealing joint and was mounted on a dynamic mechanical analyzer (Rheometric RSA-II). Measurements were performed at a frequency of 10 rad/s and at various temperatures.

Crystallization

The crystallization during polymerization was followed by DSC. Because the polymerization and crystallization are exothermic, the two phenomena must be deconvoluted.[15] However, it is possible to measure the crystallization separately by FTIR spectra.[16] The crystallization heat flow rate dH/dt was measured and the crystallinity (χ_c) calculated from

$$\frac{d\chi_c}{dt} = \frac{dH/dt}{\Delta H_f} \tag{2}$$

where ΔH_f is the overall heat of fusion (134 J/g).[17] Crystallinity measurements were performed at various temperatures between the monomer melting temperature and the final polymer melting temperature.

RESULTS AND DISCUSSION

Polymerization Kinetics

Isothermal DSC curves plotted as $d\beta/dt$ versus time are shown in Figure 3. The $d\beta/dt$ can be expressed as a function of the degree of conversion (β) and temperature (T):

$$\frac{\partial \beta}{\partial t} = C \cdot f(\beta) \tag{3}$$

$$C = K \cdot e^{-E_{act}/RT} \tag{4}$$

$$\beta = \frac{[M]_o - [M]}{[M]_o} \tag{5}$$

where $[M]_o$ and $[M]$ are the initial and time dependent monomer concentrations, respectively; K is the preexponential factor; E_{act} is the activation

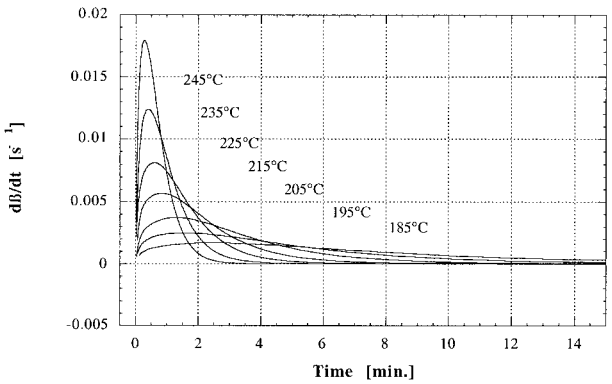

Figure 3 The reaction rate ($d\beta/dt$) versus the time at different polymerization temperatures for a 3% liquid system concentration within the monomer.

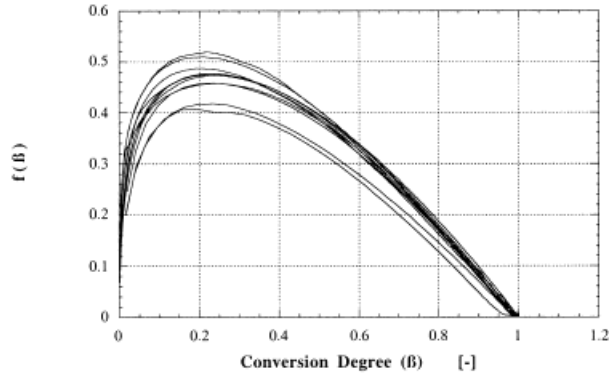

Figure 4 The determination of the kinetic function ($f(\beta)$) for temperatures ranging from 195 to 235°C and for liquid system concentrations within the monomer ranging from 3 to 6%.

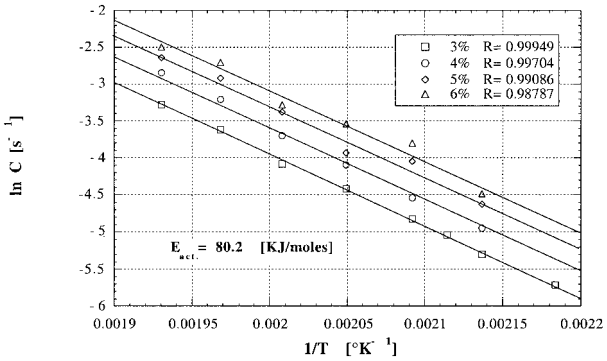

Figure 5 The rate constant C plotted as an Arrhenius graph for different temperatures and different liquid system concentrations.

energy for polymerization; and R is the gas constant.

The difficulty resided in defining the function $f(\beta)$. In the literature, activated anionic polymerization of lactam is extensively modeled for the PA6, but only occasionally for PA12. The syntheses of PA6 were modeled by either first or autocatalytic functions, whereas PA12 was by a first-order equation.[18] The authors used sodium-caprolactam as a catalyst and *N*-acetylcaprolactam as an activator. The $f(\beta)$ for PA12 was defined as

$$f(\beta) = 1 - \beta \quad \text{(first order)} \tag{6}$$

In the current work the activator composition was different as well as the activator/catalyst molar ratio. The $f(\beta)$ is plotted in Figure 4 from measurements for different temperatures and different liquid system concentrations. The function was obviously not of the first order (linear) in the entire range of conversions.

This nonlinear function should be attributed to the activator/catalyst molar ratio, which was different from unity. It was thought that the activator and the catalyst reacted to produce guanidine salt (Fig. 1), which promoted the chain reaction. Because the activator/catalyst molar ratio was 1/1.5, some unreacted catalyst remained. It was expected that the catalyst excess promoted time-differing active sites by reacting with the monomers and that these reacting sites produced a maximum of the $d\beta/dt$ versus time (Fig. 3), which was not at the beginning of the reaction ($t = 0$). In the present case, the function can be written in the following autocatalytic reaction form:

$$f(\beta) = \beta^m(1 - \beta)^n \tag{7}$$

To obtain the parameters C, m, and n the experimental data were fit with eqs. (3) and (7) by a least-squares method. This fit was performed without any other constraint on them, which meant that the overall reaction order ($m + n$) was not fixed.

The rate constant C is plotted as an Arrhenius graph in Figure 5 for different liquid system concentrations. From the linearization of eq. (4), the E_{act} and the K, corresponding respectively to the slope and the value at the temperature origin, were obtained (Fig. 5). The activation energy seemed to be independent of the liquid system concentration in that the curves had the same slope. However, the K value was dependent on the liquid system concentration. Indeed, the curves were shifted with respect to concentration variations.

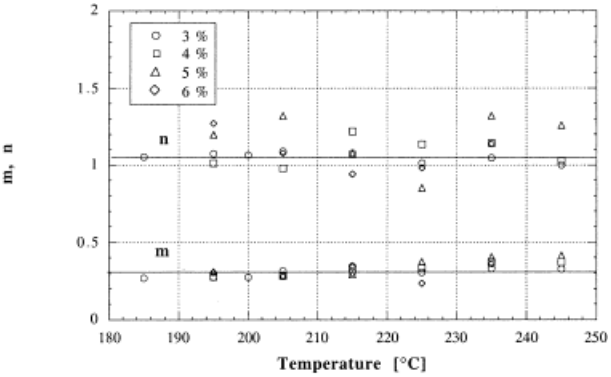

Figure 6 The m and n values obtained for different temperatures and different liquid system concentrations.

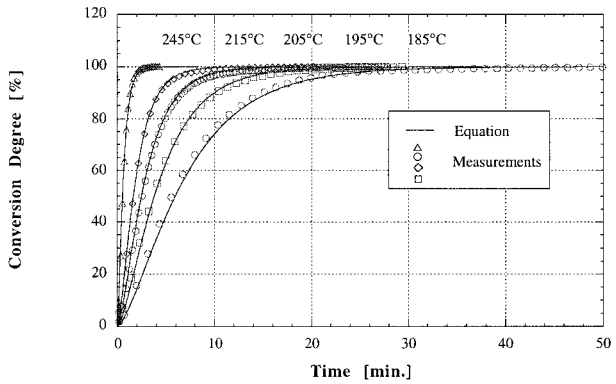

Figure 7 The experimental and calculated degree of conversion versus the time for different temperatures for a 3% liquid system concentration within the monomer.

The values of m and n obtained for each curing temperature and liquid system concentration are shown in Figure 6. These exponents were independent of the temperature and liquid system concentration change. The $m + n$ value was 1.35.

The K value was the parameter most affected by the liquid system concentration (%) and a simple linear relation seemed to occur in the measured concentration range:

$$K = (-1.816 + 2.13 \cdot [\text{liquid system}]) \cdot 10^6 \quad (8)$$

It should be noted that the K must be zero when the liquid system concentration is zero. This was not the case with the eq. (8); thus, extrapolations out of the measured concentration range were subject to caution. A similar linear relationship passing through zero was observed by Malkin.[18] He used an activator/catalyst molar ratio of 1 whereas the liquid system in the present work did not.

The β can thus be expressed versus the reaction temperature by combining eqs. (3), (4), and (7):

$$\frac{\partial \beta}{\partial t} = K \cdot \exp\left(\frac{-E_{\text{act}}}{RT}\right) \cdot \beta^m \cdot (1 - \beta)^n \quad (9)$$

where the determined parameters are $E_{\text{act}} = 80.2$ kJ/mol, $m = 0.3$, and $n = 1.05$.

Equation (8) included in eq. (9) expressed the influence of the liquid system concentration. Equation (9) was solved by a Runge–Kutta fourth-order method. Comparisons between typical experimental DSC data and predictions of the model are shown in Figure 7.

The overall heat involved in the reaction was determined as the average value of reaction heats calculated in each thermogram. The corresponding values found were $\Delta H_o = -53$ J/g $\pm$ 3%. This value was fully consistent with the -53.8 J/g found in a recent study.[19] Previous sources gave reaction exotherms of -66 and -43 J/g.[20,21]

The kinetics study enabled the prediction of the β versus the time, temperature, and liquid system concentration. The results were used for designing processing techniques to produce PA12 parts in short amounts of time.

Melting Temperatures

Typical DSC measurements of monomer and polymer melting peaks are shown in Figure 8 as a function of the polymerization evolution. The polymer melting temperature increased versus the time whereas the monomer melting temperature decreased.

The typical final melting temperature of this specific PA12 was 174°C. This value corresponded to the melt of crystallites developed on cooling.

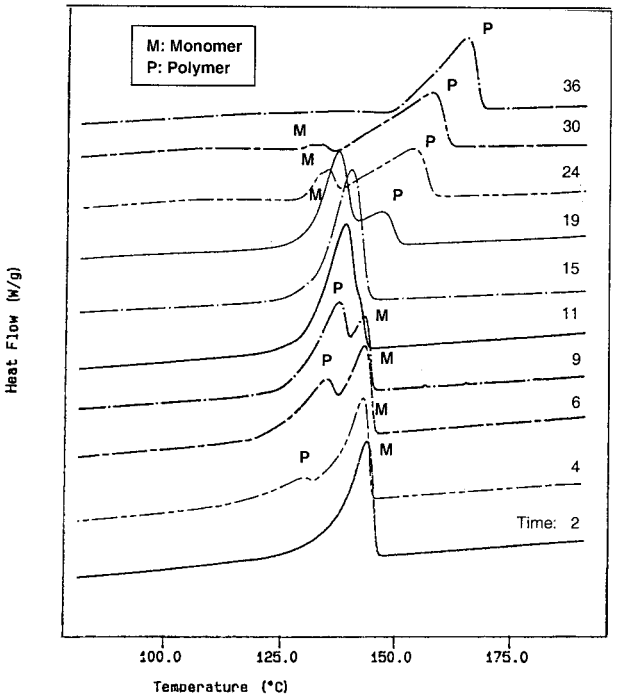

Figure 8 Typical DSC measurements of melting temperatures at different degrees of conversion (i.e., different times). The polymerization temperature was 166°C.

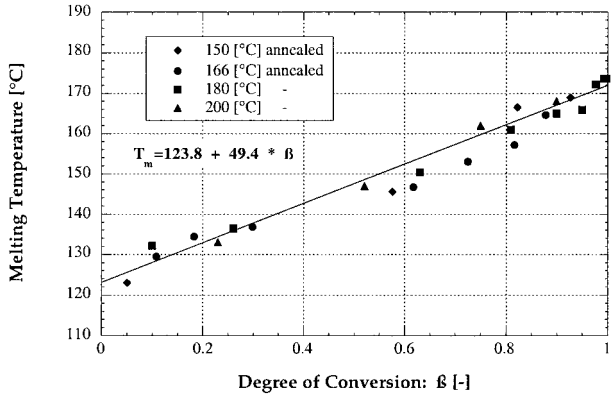

Figure 9 The final melting temperatures versus the degrees of conversion. The samples were polymerized at different temperatures and remelted when the polymerization temperature was below 174°C.

However, crystallites formed during polymerization can lead to much higher melting temperatures. At polymerization temperatures above the final melting point (174°C) the only crystallization that occurred was during cooling, and the maximum melting point was thus 174°C. In contrast, below the final melting point, crystallization during polymerization also occurred[22] and it increased the maximum melting point. This effect could be suppressed by annealing the sample. The melting temperatures versus the β are plotted in Figure 9 for the annealed samples. The relation was almost linear for all polymerization temperatures.

In our case, two mechanisms influenced the melting temperature change versus the β: the molecular weight and the solvent. The solvent concentration change was due to monomer consumption. The molecular weight can be calculated from the β as follows:

$$\overline{M}_n = X_n M_L \tag{10}$$

where $\overline{M}_n$ is number-average molecular weight M_L is the molecular weight of one PA12 monomer, and X_n is the number-average degree of polymerization, which is defined as

$$X_n = \beta[M]_o/[A^*]_o \tag{11}$$

where $[A^*]_o$ is the initial active species concentration. These formulae assumed that each molecule of an active species in the liquid system (Fig. 1) was a center of the macromolecule growth. In the present work the M_n reached 59,000 after all monomers were consumed. The volume fraction of the solvent v_1 can be calculated as

$$v_1 = \frac{(1-\beta)\cdot\rho_{\text{mon}}}{(1-\beta)\cdot\rho_{\text{mon}} + \beta\cdot\rho_{\text{pol}}} \tag{12}$$

where ρ is the density of the monomer and the polymer. During polymerization the molecular weight increased and the solvent concentration decreased. Their influence on the melting temperature, according to the work of Flory et al.,[23,24] should be expressed as the molecular weight effect,

$$\frac{1}{T_m} - \frac{1}{T_m^i} = \frac{2R}{\Delta H_u X_n} \tag{13}$$

and the solvent effect,

$$\frac{1}{T_m} - \frac{1}{T_m^*} = \frac{R}{h_u}\cdot\frac{V_2}{V_1}\cdot(v_1 - \chi v_1^2) \tag{14}$$

where T_m^i is the melting point for infinite molecular weight; ΔH_u is the heat of fusion per monomer unit; T^*_m is the absolute melting temperature of the polymer (of high molecular weight) in the absence of diluent; h_u is the heat of fusion per mole of structural unit; V_2 and V_1 are the molar volumes of the polymer unit and the diluent molecules, respectively; and χ is the Flory–Huggins interaction parameter, which is characteristic of a given polymer–diluent pair.

In order to evaluate the predominance of one mechanism over the other, eqs. (13) and (14) were fitted to the measurements. The equation related to the solvent showed the best fit and was obtained with a χ of zero, which could be expected because of the chemical similitude of the monomer and the polymer. However, the predominance of the solvent effect was not well established. The poor fit of the equation related to the molecular weight might have resulted from a significant deviation from linearity at a large degree of conversion. That was indeed revealed by Evans et al.[23] for smaller polymerization degrees than in the current work.

The relationship measured between the melting temperature and the conversion degree (Fig. 9) was thus empirical. This relationship was used for isomelting curve calculations.

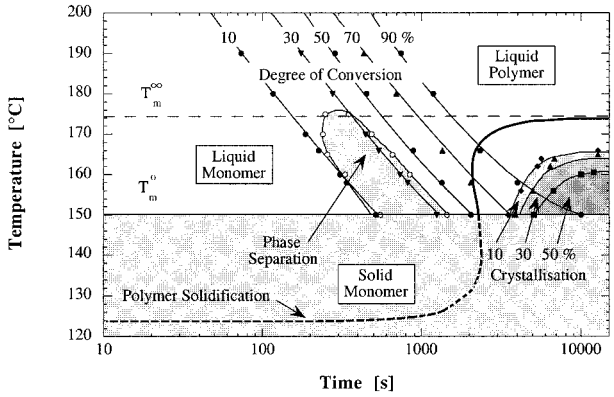

Figure 10 The full range of isoconversions and phase transformations versus the time and temperature during the polymerization. The horizontal lines show the melting point of the monomer (150°C) and of the polymer (174°C).

Phase Transformation Diagram

The same approach that existed for thermosets[10,11,25,26] was used to build a TTT diagram. Because thermoplastic polymers are linear molecules, no gelification in the sense of thermosets would ever occur. However, vitrification might happen when the glass-transition temperature (T_g) of the resin is higher than the curing temperature. In the case of PA12, the diagram dealt with melting temperatures rather than with the T_g. Indeed, PA12 is a semicrystalline polymer and its monomer is fully crystalline. The diagram for thermoplastic polymers shown in Figure 10 was built by isothermal measurements. The melting point of the monomer (T_m^o) and the final melting point of the polymer (T_m^∞) are indicated by two horizontal lines at 150 and 174°C, respectively. The other curved lines correspond to seldom successive conversion degrees from 10 to 90%. They show the time needed to reach a given degree of conversion at different temperatures. Below the melting point of the monomer, no reaction can occur and the isoconversion lines have a discontinuous slope change. A phase separation of the polymer and its monomer occurred between 10 and 30% of the β. These data were obtained at equilibrium by turbidity measurements according to Malkin.[27]

Crystallization attributable to polymerization took place below the final polymer melting temperature. Indeed, the polymerized fraction started to crystallize whereas the monomer remained molten. The curves on the right of the Figure 10 represent 10, 30, and 50% of the crystallinity. At low temperatures, where the induction time of crystallization was short, crystallization and polymerization occurred at the same time. Therefore, a competition between the polymerization rate and the crystallization rate occurred at each temperature, but it must be kept in mind that only the polymerized fraction could start to crystallize. Crystallization had a strong effect on the reaction kinetics and the final β. The $d\beta/dt$ was strongly decreased and thus the isoconversion lines were extended to longer times when they overlapped crystallization. This can be explained by the fact that some polymerization nuclei were caught in the crystalline parts and the overall reactivity was decreased. To avoid this polymerization rate decrease, the polymerization must be completed before crystallization starts. This can be performed by working above the final melting point of the polymer or by having a fast polymerization. It is important to remark that the reaction exotherm can be exploited to reach a higher temperature than the final melting point. In the PA12 with a measured enthalpy of -53 J/g, it was determined that the reaction in fully adiabatic conditions led to an increase of only 20°C.

Crystallization had a second effect on polymerization: it increased the final degree of conversion. Indeed, the crystal fraction was not involved in the polymer–monomer equilibrium[28] because the crystallized fraction of the polymer was protected from depolymerization. Thus, the final concentration of the monomer was shifted to a lower value.

Without this crystallization effect the equilibrium monomer content can be calculated from the enthalpy and entropy of the reaction. A negative enthalpy was found in the present work. The polymerization entropy was more difficult to measure. Bonetskaya and Skuratov[29] overestimated it by extrapolation. Their results were reported in subsequent work.[30] The best reliable entropy value is from Aharoni.[31] He extracted the values from the results obtained experimentally by Sebenda[32] who studied PA6 equilibra with cyclic oligomers of caprolactam with different ring sizes. He obtained a value of $\Delta S = 28.1$ J/K mol.

Subsequently, by assuming a positive entropy and according to the Gibbs equation, $\Delta G = \Delta H - T\Delta S$, we concluded that polymerization took place at all temperatures (i.e., <0 at all temperatures). There was thus no ceiling or floor temperature and no depolymerization should take place at high temperatures, even for long amounts of time, as long as no other reactions occurred (oxidation, crosslinking).

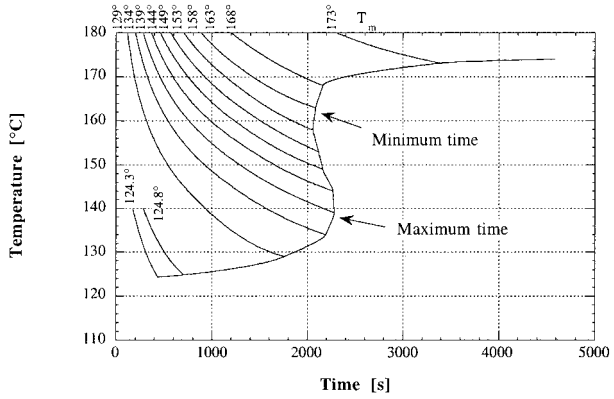

Figure 11 The establishment by isomelting points of the times where the melting point of the polymer reached the polymerization temperature.

The S-shaped curve (polymer solidification) in Figure 10 corresponds to the time at which the melting point of the polymer was equal to the polymerizing temperature. No polymer crystallization could occur above the curve. Below the curve, when the melting point of the polymer was higher than the polymerization temperature, crystallization could take place. The construction of the polymer solidification curve is presented in Figure 11. The points where the isomelting temperature curves equalled the polymerization temperature ($T_m = T_{\text{polymerization}}$) were joined. The isomelting temperature curves were calculated from the isoconversion curves with the equation in Figure 9. The part of the polymer solidification curve (Fig. 10) below the monomer melting point is fictive, because no polymerization occurred at that temperature.

The minimum time to this curve (Fig. 11) was a consequence of the opposing influence of the temperature on the $d\beta/dt$ increase and on the monomer concentration decrease. Indeed, the reaction accelerated with the temperature augmentation but following this extent of temperature on the curve we see that the conversion degree rose (Fig. 10), inducing the decrease of the $d\beta/dt$ (Fig. 4). Between 140 and 160°C the chemistry kinetics controlled the shape of the curve: the $d\beta/dt$ increased with the temperature and the time to the curve decreased. Above 160°C the effect of the monomer motion started to be dominant as the β at the curve was growing. Thus, above 160°C the time to the curve increased.

The maximum time to the curve in Figure 11 can be considered to be due to the influence of temperature on the $d\beta/dt$ and to the fact that the melting temperature of the first polymerized product was 124°C (Fig. 9).

No vitrification was observed with PA12 because no polymerization took place below the monomer melting temperature (T_m^o) and the final glass transition (T_g^∞) was below the monomer melting temperature. To observe vitrification, the glass transition of the polymer should reach the polymerization temperature. This was possible during polymerization of PA4 and PA3 from pyrrolidone and propiolactam, respectively. Indeed, their T_g^∞ was above the lowest possible polymerization temperature, which was the T_m^o.

Chemorheology

Because the viscosity increased as the polymerization progressed, a maximum available time existed to impregnate the fibers. A full and homogenous impregnation was required for good composite properties. Therefore, it was important to predict this available time and to compare it with the required time for processing. The available time depended on the reaction kinetics and thus on the temperature, whereas the required

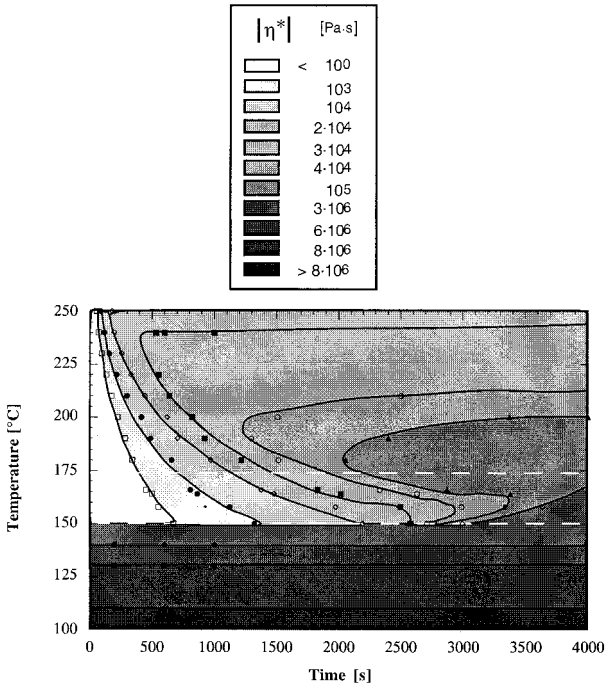

Figure 12 The full range of isoviscosities versus the time and temperature during polymerization. The white dashed lines show the melting point of the monomer (150°C) and of the polymer (174°C).

time depended on pressure, fiber permeability, and the path length that the resin had to flow. Figure 12 presents isoviscosity curves versus the time and temperature. They were measured isothermally. The curve at 1 Pa s allows one to read the available impregnation time versus temperature if we estimate that the flow practically stops when the viscosity becomes greater than 1 Pa s. The melting temperature of the monomer and the final melting temperature of the polymer are represented by the two white dotted lines. Above the final polymer melting temperature, the viscosity increase was uniquely attributable to the β increase. However, because the viscosity was also temperature dependent, there was a maximum viscosity for each temperature. This explained the minimum time for an isoviscosity curve at high temperature.

Below the final polymer melting temperature and with short amounts of time the viscosity increase was due to the polymerization; at longer periods of time the viscosity increase was also due to the crystallization. The maximum time to an isoviscosity curve below the final melting temperature of the polymer was due to the opposing influence of the temperature dependence of the crystallization rate and the $d\beta/dt$. It should be noted that the phase separation that was revealed in the TTT diagram did not seem to have significant influence on the viscosity measurement.

Processing Route Through Phase Diagram

The aim of the TTT diagram is to provide various processing routes to fully exploit *in situ* polymerization. The potential applications of these thermoplastic diagrams are not exactly the same as the ones for thermosets,[11] because the encountered events are not the same. However, crystallization for thermoplastics, as well as vitrification for thermosets, strongly decreased the $d\beta/dt$. Furthermore, the control of the thermoplastic reaction exotherm should then be possible in the same way as for thermosets[11] by the control of the $d\beta/dt$.

Fast and full polymerization could be achieved above and below the final polymer melting temperature (T_m^∞) if the reaction was completed before crystallization starts. When processing the material at high temperatures, the polymerization could be faster and phase separation was avoided.

Below the final polymer melting temperature the maximum equilibrium conversion degree was obtained, even in cases where crystallization started before the end of polymerization, but this occurred at slow polymerization rates. This later approach was used for PA6, although the processing temperature increased because of the reaction and crystallization exotherms.[28]

Crystallization induced by polymerization might be interesting as a way to decrease internal stresses. At processing temperatures below T_m^∞ and by postulation of quasi-adiabatic conditions, the formed polymer would solidify throughout the whole mass before cooling without development of internal stresses.

Processing routes can be chosen to improve the final β. It was shown that the crystalline fraction of the polymer being formed did not participate in the polymer–monomer equilibrium.[28] Therefore, for a given polymer, the residual monomer equilibrium content can be shifted to lower values by the choice of a processing temperature lower than the polymer melting point. The lowest polymerization temperature is determined by the monomer melting point or by the polymer–monomer insolubility effect. The association of crystallization and polymerization thus might open new processing routes for thermoplastics having a poor final β. A full degree of conversion is needed, because the residual monomer diffuses to surfaces of the parts. This is in contrast to thermosets where a maximum conversion is not needed. Indeed, the final properties of the thermoset can be controlled by the crosslink density. The design of thermoplastic partially reacted preforms (e.g., prepreg) will be limited as long as polymerization reactions remain sensitive to exposure to water from the surrounding air.

Information on cooling of thermoplastics is missing in the TTT diagrams. Crystallization appeared not only during polymerization but also during cooling. To process a thermoplastic by *in situ* polymerization, information regarding the influence of the cooling rate on the final crystal content should be collected. In the current case, preliminary results showed that the PA12 crystallinity was not much affected by the process cooling rates.[33]

The kinetics and chemorheology results are currently being applied to the processing of PA12 composites using pultrusion, resin transfer molding,[12] and rotomolding.

CONCLUSION

Several time–temperature routes were determined for the reactive processing of PA12 composites, and the kinetics and chemorheology of a novel activator/catalyst system were presented. Complete polymerization was achieved above and below the T_m^∞. Rapid polymerization could be obtained either above or below the T_m^∞ if the reaction was completed before the onset of crystallization. The material transformations occurring during polymerization were described and summarized in a TTT diagram. Although in thermosets the crosslink density can be controlled, a full β was required for thermoplastics to avoid the residual monomer diffusing to the part's surface. It was thus impossible to control the final properties of the PA12 by controlling the degree of conversion and the reaction temperatures. However, the final properties could be controlled by the initial concentrations of the activator and catalyst, which influenced the molecular weight, and by the cooling rate, which influenced the crystallization. On the other hand, using a processing temperature lower than the polymer melting temperature could improve the processability of certain thermoplastics that presently have a poor final β.

The authors would like to thank EMS CHEMIE AG and EBO for their support and collaboration. The financial support of the Commission for Technology and Innovation (CTI) is also highly appreciated.

REFERENCES

1. Månson, J.-A. E. New Demands on Manufacturing of Composite Materials, TMS/ASM High Performance Composites; Rosemont, IL: TMS, 1994.
2. Chen-Chi, M. M.; Chin-Hsing, C. Polym Eng Sci 1991, 31, 1086.
3. Dubé M. G.; Batch, G. L.; Vogel, J. H. Polym Compos 1995, 16, 378.
4. Chen, C.-H.; Wang, W.-S. Polym Compos 1998, 19, 415.
5. Ishida, H. Eur. Pat. 0 384 063 A2, 1989.
6. Binse, P. Eur. Pat. 0 544 049 A1, 1991.
7. Chen, J.-H.; Kang, C.-J.; Wu, Y.-D.; Laiw, R.-F. U.S. Pat. 5,424,388, 1995.
8. Cho, B.-G.; Mc Carty, S. P.; Fanucci, J. P.; Nicolet, S.C. In Proceedings of the 24th International SAMPE Technical Conference, Toronto, Canada, 1992.
9. Joyce, R. M.; Ritter, D. M. U.S. Pat. 2,251,519, 1941.
10. Enns, J. B.; Gillham, J. K. J Appl Polym Sci 1983, 28, 2567.
11. Simon, S. L.; Gillham, J. K. J Appl Polym Sci 1994, 53, 709.
12. Connor, M.; Eder, R.; Schmid, E.; Wild, U. EMS Polymerization Molding (EPM): A Novel Solution to Thermoplastic Composite Manufacturing, Progress Through Innovation and Cost Effectiveness; Paris: SAMPE Europe, 1998.
13. Schmid, E.; Eder, R. Ger. Pat. DE 19602684 C1, 1997.
14. Luisier, A. Ph.D. Thesis, Swiss Federal Institute of Technology, Lausanne, 2000.
15. Karger-Kocsis, J.; Kiss, L. Makromol Chem 1979, 180, 1593.
16. Ishida, H.; Scott, C. J Polym Eng 1986, 6, 201.
17. Stamhuis, J. E.; Pennings, A. J. Polymer 1977, 18, 667.
18. Malkin, A. Y.; Ivanova, S. L. Polymer 1982, 23, 1791.
19. Franze, T. M.; Kolelnikov, V. A.; Ivanov, M. P.; Danilevskaya, L. B.; Davtyan, S. P.; Korshak, V. V. Dokl Akad Nauk SSSR Chem 1981, 260, 1379.
20. Elias, H. G.; Fritz A. Makromol Chem 1968, 114, 31.
21. Malkin, A. Y.; Ivanova, S. L.; Korchagina, M. A. Vyskomol Soed Ser A 1977, 19, 2224.
22. Wunderlich, B. Fortschr Hochpolym-Forsch 1968, 5, 568.
23. Evans, R. D.; Mighton, H. R.; Flory, P. J. J Am Chem Soc 1950, 72, 2018.
24. Mandelkern, L.; Flory, P. J. J Am Chem Soc 1951, 73, 3206.
25. Simon, S. L.; Gillham, J. K. J Appl Polym Sci 1993, 47, 461.
26. Wisanrakkit, G.; Gillham, J. K.; Enns, J. B. J Appl Polym Sci 1990, 41, 1895.
27. Malkin, A. Y. A. Polym Eng Sci 1980, 20, 1035.
28. Wichterle, O.; Sebenda, J.; Kralicek, J. Fortschr Hochpolym-Forsch 1961, 2, 578.
29. Bonetskaya, A. K.; Skuratov, S. M. Polym Sci USSR 1969, 11, 604.
30. Sekiguchi, H. In Ring-Opening Polymerization; Ivin, K. J., Saegusa, T., Eds.; Elsevier: New York, 1984; Vol. 2, p 1133.
31. Aharoni, S. M. *n*-Nylons: Their Synthesis, Structure and Properties; Wiley: New York, 1997.
32. Sebenda, J. Pure Appl Chem 1976, 48, 329.
33. Zanetto, J.-E. Ph.D. Thesis, Swiss Federal Institute of Technology, Lausanne, 2000.